

AN ARRHYTHMIA CLASSIFICATION-GUIDED SEGMENTATION MODEL FOR ELECTROCARDIOGRAM DELINEATION

CHANKYU JOUNG¹, MIJIN KIM², TAEJIN PAIK¹, SEONG-HO KONG^{3,4}, SEUNG-YOUNG OH^{4,5},
WON KYEONG JEON⁶, JAE-HU JEON⁷, JOONG-SIK HONG⁷, WAN-JOONG KIM⁷,
WOONG KOOK^{1,3}, MYUNG-JIN CHA², OTTO VAN KOERT^{1,3},

ABSTRACT. Accurate delineation of key waveforms in an ECG is a critical initial step in extracting relevant features to support the diagnosis and treatment of heart conditions. Although deep learning based methods using a segmentation model to locate P, QRS and T waves have shown promising results, their ability to handle signals exhibiting arrhythmia remains unclear. In this study, we propose a novel approach that leverages a deep learning model to accurately delineate signals with a wide range of arrhythmia. Our approach involves training a segmentation model using a hybrid loss function that combines segmentation with the task of arrhythmia classification. In addition, we use a diverse training set containing various arrhythmia types, enabling our model to handle a wide range of challenging cases. Experimental results show that our model accurately delineates signals with a broad range of abnormal rhythm types, and the combined training with classification guidance can effectively reduce false positive P wave predictions, particularly during atrial fibrillation and atrial flutter. Furthermore, our proposed method shows competitive performance with previous delineation algorithms on the Lobachevsky University Database (LUDB).

1. INTRODUCTION

An electrocardiogram (ECG) is a basic medical diagnostic tool that monitors the electrical activity of the heart. It is non-invasive, relatively quick to perform, inexpensive, and provides a wealth of valuable information about the overall health of the heart. Traditionally, the analysis of the structural elements in an ECG, including the durations and morphology of the QRS complex, the P and T waves (see Figure 1), plays a key role in identifying abnormalities or irregularities in the heart’s electrical activity that may point towards underlying heart conditions [1]. Therefore, precise delineation, which involves identifying the onset and offset of these waves, is critical.

Computerized interpretation of ECGs has been available since the 1950s and has enabled the automatic delineation of ECG features. Over time, significant improvements have been made in the quality of automatic delineation using various techniques. Among these techniques, wavelet transform-based delineation [2, 3, 4] is widely recognized as one of the most effective, delivering state-of-the-art performance on the benchmark QT database (QTDB) [5]. However, as pointed out by [6, 7], these methods often require the adjustment of a threshold value to attain high scores, which may limit their generalizability to other datasets.

In recent years, deep learning has shown remarkable success in ECG processing such as arrhythmia classification [8], which led to its increasing popularity in various downstream tasks [9]. This has been the case for ECG delineation as well, where a segmentation model with a CNN architecture is typically trained to locate the P, QRS and T waves, which is then used to carry out the delineation task. For instance, Jimenez-Perez et al. [6] used a U-Net architecture [10] for their segmentation model, achieving delineation performance

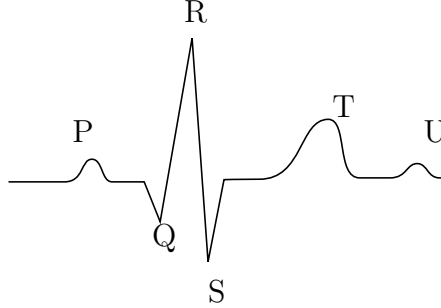


FIGURE 1. A schematic representation of an ECG signal measured in lead I or lead II with the main complexes indicated.

comparable to wavelet-based methods on QTDB. Similarly, Moskalenko et al. [11] employed a U-Net architecture and reported higher delineation performance compared to wavelet-based algorithms on the Lobachevsky University Database (LUDB) [12].

Despite the progress made, accurate delineation of an ECG signal during arrhythmia still remains a challenge. Many arrhythmias cause significant changes in the structural elements and morphological features of an ECG. This is most notably the case for the P wave, which usually has the lowest signal to noise ratio. For example, in atrial fibrillation (AFIB) and atrial flutter (AFL) the P wave is absent, and a fibrillatory signal or flutter wave is found instead. As noted in [13] and [14], false P wave predictions during such events present a significant challenge for delineation algorithms in clinical practice. Other arrhythmias, such as atrioventricular (AV) block, affect not only the position of P waves in relation to the QRS complex, but also their occurrence. This can result in P waves and QRS complexes following independent rhythms. In all of these cases, the performance of a P wave delineation algorithm is affected adversely. For instance, Aziz et al. [15] report a considerable drop in sensitivity for P wave detection in the case of ECGs exhibiting arrhythmia.

A related challenge in deep learning based ECG segmentation is the scarcity of high-quality annotated data required for supervised training of models. To the best of our knowledge, the QT Database (QTDB) [5] and Lobachevsky University Database (LUDB) [12] are currently the only publicly available databases that provide onset and offset annotations for all P, QRS and T waves in multiple leads. As a result, the training and validation of previous segmentation models have primarily been restricted to these datasets. For example, Jimenez-Perez et al. [6] carried out a 5-fold cross validation using the 105 patients in QTDB, while Moskalenko et al. [11] trained their model on the extended LUDB dataset, which includes 455 patients. Although these models achieved high accuracy on their respective test sets, also sourced from QTDB and LUDB, it remains uncertain how they would perform on individual arrhythmia types that are not represented in the limited training data.

In this paper, we propose a new deep learning based approach in the form of arrhythmia classification-guided segmentation, as depicted in Figure 2. Our approach involves designing a segmentation model by adding a separate classification branch to a standard encoder-decoder architecture. The model is then trained with a combined loss for both segmentation and classification. This method allows the model to learn features related to the heart rhythm and to accurately delineate various arrhythmias. For short ECG signals, the classification output can be used to suppress false P wave predictions in the segmentation result. We have adapted this classification-guided approach from previous research on medical image

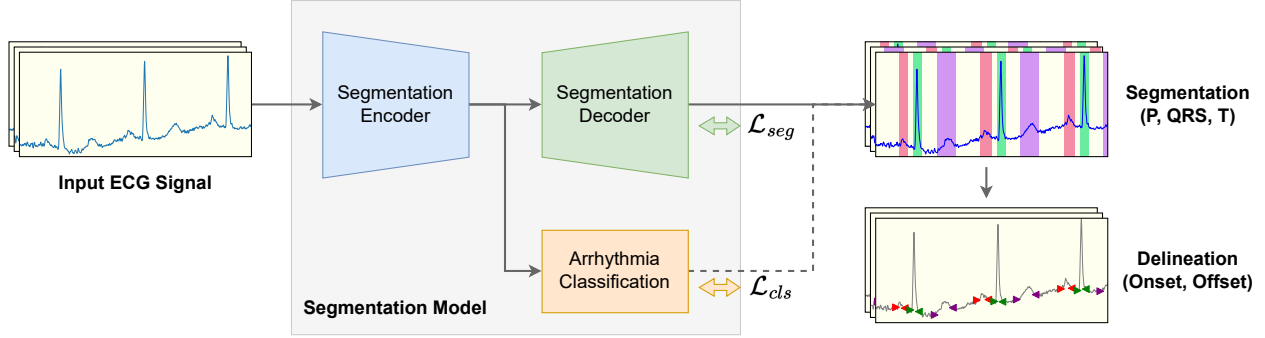


FIGURE 2. Schematic diagram of the proposed ECG delineation method.

segmentation [16,17] and applied it to train an ECG segmentation model, with arrhythmia classification as the additional classification task.

In addition, we created an internal dataset with a controlled distribution of various arrhythmia types. The dataset comprises 1557 unique patients, significantly larger than both QTDB (150 patients) and LUDB (200 patients). The dataset includes a large number of patients with arrhythmias such as Atrial Fibrillation (155 patients) and Atrial Flutter (59 patients). By training the model on this dataset combined with the previously mentioned classification loss, it can explicitly learn to handle a wide range of morphological behavior that a signal can display during arrhythmia events. Moreover, this dataset provides us with an opportunity to evaluate the model’s performance separately on different arrhythmias, enabling a detailed quantitative analysis that is not feasible when evaluating only on the current public datasets such as QTDB and LUDB.

We performed experiments on three tasks. First, we evaluated the segmentation model’s performance on the internal dataset to showcase its ability to delineate various arrhythmias. The results show that the number of false P wave predictions can be notably reduced by the proposed classification-guided method. We also observed that the distribution of arrhythmias in the training set can significantly influence segmentation performance, particularly for abnormal rhythm types. Second, we compared the performance of our model with previous benchmark models by evaluating it on the LUDB dataset. Despite being trained on a separate internal dataset, our model surpassed previous deep learning based methods in F1 score, demonstrating its ability to generalize to unseen datasets. Finally, we conducted a visual demonstration of our model’s segmentation capabilities by applying it to long ECG recordings in the MIT-BIH arrhythmia database [18].

2. RELATED WORK

2.1. Traditional Approaches for ECG Delineation. Early works on ECG delineation were primarily focused on developing rule-based methods to identify and locate the QRS complex. Pan and Tompkins [19] presented a seminal example of detecting the QRS complex by utilizing slope, amplitude, and width information. Subsequently, more advanced techniques have been employed to identify also the P and T waves. These include digital signal processing such as the wavelet transform [2,3,4], the Hilbert transform [20,21], and the phasor transform [22]. Additionally, classical machine learning approaches like hidden Markov models [23,24] and Gaussian mixture models [25] have also been employed. Among these, wavelet-based methods have been widely cited as being the state-of-the-art, based on their

delineation performance on the public dataset QTDB. Recently, the wavelet based algorithm proposed by Kalyakulina et al. [4] has been validated on the LUDB dataset as well.

2.2. Deep Learning based ECG Segmentation. In recent years, the application of deep learning techniques has provided an alternative for the automatic delineation of ECG signals. Typically, a segmentation model based on an encoder-decoder structure is developed, which can effectively detect the regions associated with P, QRS and T waves by proper training. Jimenez-Perez et al. [26] presented an adaptation of the U-Net architecture [10] to 1-dimensional data, while Sereda et al. [27] deployed an 8-layer convolutional network and studied the effects of using an ensemble of networks as opposed to using a single network for the segmentation. Recently, Moskalenko et al. [11] developed a U-Net-like architecture that achieved state-of-the-art performance on LUDB in terms of F1-score, when compared to previous deep learning approaches [27] and wavelet-based methods [4]. In a similar study, Jimenez-Perez et al. [6] again adapted a U-Net for segmentation but with added emphasis on regularization techniques for training with limited data. Their model, when cross-validated on QTDB, demonstrated comparable performance to those using digital signal processing techniques such as wavelet transforms [3]. Our approach is in line with both [11] and [6], but we combine segmentation with classification guidance, which we discuss next.

2.3. Classification Guided Segmentation. In developing a neural network for semantic segmentation, it is sometimes beneficial to add an extra classification task. This approach has been particularly effective in the field of medical image segmentation, where detection of false positives is common for images in which the object of interest is not present. Huang et al. [16] addressed this problem of over-segmentation by introducing a classification guided module (CGM) where the model is trained with the additional classification objective of deciding whether or not a given image contains an organ. By filtering out the segmentation output using the classification output, the number of false positives is reduced. A similar approach was taken by Shuvo et al. [17], where a separate localizer branch was added together with an additional classifier branch.

In the ECG literature, classification and segmentation tasks have remained separate for the most part, while deep learning architectures have shown great success for both tasks [9]. In our current work, we combine these two tasks by training an ECG segmentation model together with an additional arrhythmia classification learning objective. Previous studies have demonstrated the effectiveness of convolutional neural networks for arrhythmia classification. For example, Hannun et al. [8] trained a 34-layer convolutional neural network for arrhythmia classification of single-lead ECG signals, showing performance comparable to that of cardiologists. Ribeiro et al. [28] later used a residual network architecture, an architecture first developed by He et al. [29] in the context of image classification, for the reliable diagnosis of 12-lead ECG signals.

3. METHODS

3.1. Segmentation Model. Our model follows the encoder-decoder structure of U-Net [10], and we have adapted it as in previous papers [6, 11, 27] to work in the context of ECG signals. The high-level architecture is shown in Figure 3.

The encoder takes a raw ECG signal of 500Hz as input and encodes it into feature maps at multiple levels through a series of 1D convolutional blocks. Each block is followed by a MaxPool layer which downsamples the input by a factor 2. The decoder, which also consists

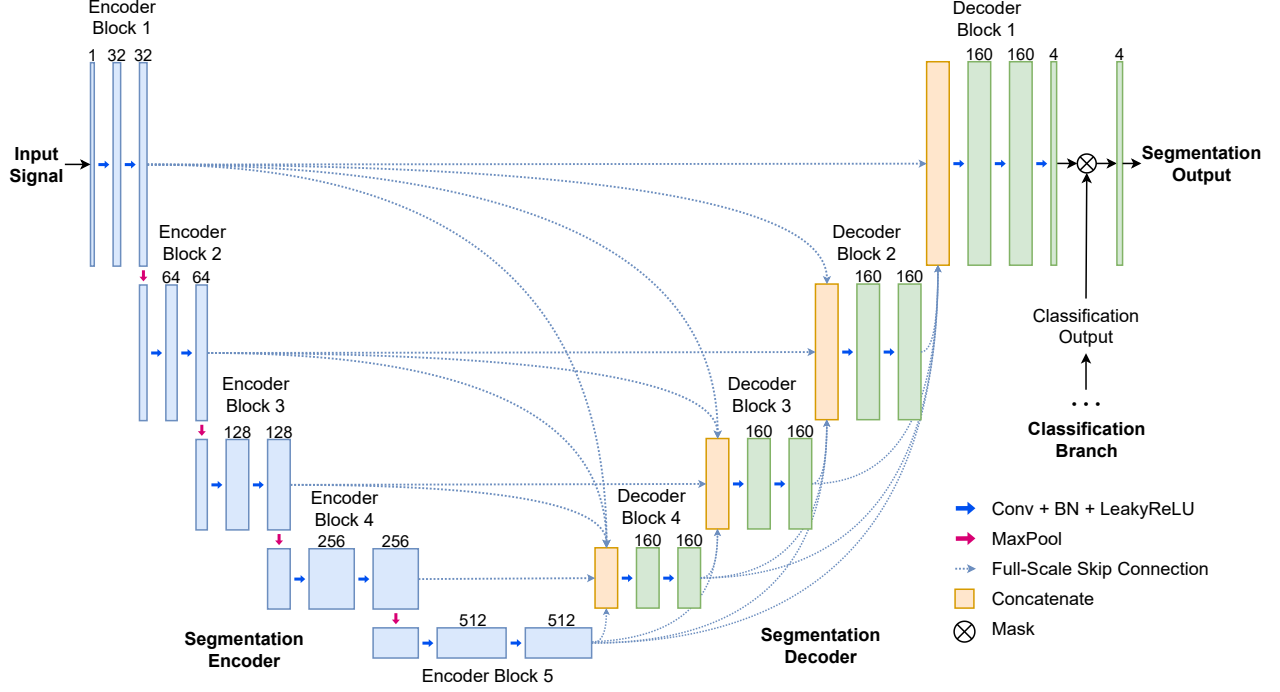


FIGURE 3. Segmentation model architecture.

of convolutional blocks but uses linear interpolation layers instead of pooling, combines and transforms these features into a final segmentation output, consisting of four channels. Each of these four channels corresponds to a probability value indicating the likelihood that the signal at a specific timestamp belongs to the P wave segment, the QRS complex segment, the T wave segment or none of these.

To further enhance the segmentation ability, we allow the decoder networks to learn from and aggregate features coming from multiple levels, by adapting re-designed skip connections of the U-Net variants [16,30]. These studies show that the performance improves by enabling the decoder to access both high-level and low-level semantics learned from the previous encoder and decoder networks. In particular, we chose to implement the full-scale skip connections of [16], which has the advantage of incorporating encoder and decoder feature maps from all scales to each decoder layer, while retaining efficiency due to a relatively small number of parameters.

The skip connections are designed as follows. Each decoder block receives feature maps directly from encoder blocks at the same or at a lower level, together with the feature maps from all the previous decoder blocks. These five feature maps are either upsampled or downsampled to be of the same resolution as the feature map from the same level encoder, by applying linear interpolation or MaxPool. They are then passed through a 1D convolutional layer with 32 filters. The resulting five feature maps from different levels, which are now of equal shape, are concatenated, then aggregated by a final convolutional block with 160 filters, which gives the decoder output.

The output of the final decoder is passed through a convolutional layer with 4 filters and kernel size 1, and then fed to a multi-class softmax classifier to produce class probabilities for each time stamp. Note that for all other convolutional layers, we use a kernel size of 9

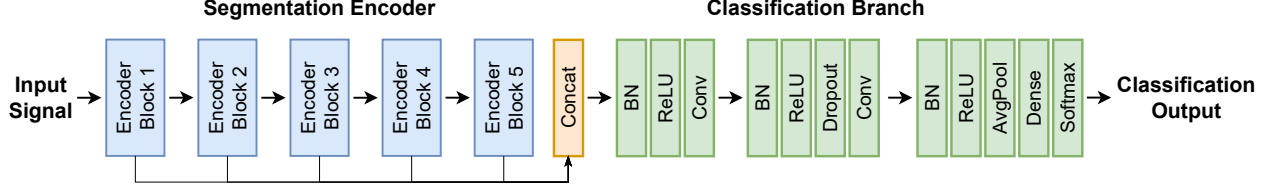


FIGURE 4. Arrhythmia classification branch network architecture.

and padding of 4. As for the activation function, we use a leaky rectified linear unit with negative slope 0.01 for all layers.

3.2. Arrhythmia Classification Guidance. To accurately delineate ECG signals with arrhythmia, it is beneficial to have explicit knowledge of the arrhythmia type a given signal belongs to. For instance, the knowledge of whether a given signal belongs to an atrial fibrillation event or not can allow the model to distinguish fibrillatory waves from P waves with more ease. In this regard, previous advanced rule based approaches to P wave detection such as [13] have incorporated atrial fibrillation classification directly in the algorithm’s decision process.

Here, we choose to train the segmentation model jointly with a classification loss based on the arrhythmia type of each input signal. The effect of this is twofold. Firstly, by training the model for classification, we allow the model to learn semantic information (such as absence of P waves) which is relevant to but not explicitly required for the segmentation task. Secondly, we can directly suppress the P wave segmentation output when a short signal is predicted to belong to, for instance, an atrial fibrillation episode. This allows us to reduce the number of false positive P waves in a convenient manner. To jointly train segmentation with classification, we add a classification branch following the deepest layer of the encoder. This is similar to the classification guided modules of [16, 17], which have been used in the context of biomedical image segmentation. Here, we re-design the structure for the task of arrhythmia classification of ECG signals.

The structure of the arrhythmia classification branch is shown in Figure 4. The classification branch itself consists of two convolutional layers. Each convolutional layer has 512 filters and uses kernel size of 17. In between the convolutional layers, we apply batch normalization and a ReLU non-linearity. We also apply Dropout before the second convolutional layer. The arrhythmia classification is performed by the final fully connected layer with softmax activation. The output represents the probabilities of the signal belonging to either an atrial fibrillation/flutter episode or not. A final prediction is made using an argmax function. During evaluation on 10 second ECG signals, we can then directly suppress the P wave segmentation output when the signal is predicted to correspond to atrial fibrillation or atrial flutter.

Note that we have allowed the classification branch to take as input not just the feature of the last encoder block, but of encoder blocks of all levels. This is done by an aggregation scheme which works as follows. We first downsample the features of the first four encoder blocks to a size equal to that of the last encoder block. The downsampling is done using an average pooling layer. After the features have been resampled to the same shape, we concatenate the features to get a single aggregated feature. By passing in the aggregated feature into the following layers, we allow the classification to be performed using both high-level and low-level features.

Data Source	# Patients	Duration	Frequency	Leads	Annotations
Internal Database	1557	10 seconds	500Hz, 250Hz	2 (I, II)	P, QRS, T on/offsets
LUDB [12]	200	10 seconds	500Hz	12	P, QRS, T on/offsets

TABLE 1. Descriptions of signals and their annotations for each of the databases.

3.3. Loss Function. One important aspect of ECG segmentation which needs to be taken care of is the difference in difficulty between the classes: P, QRS and T waves. This is partially due to their morphological characteristics. For instance, P waves usually have a lower amplitude than the other two, and are hence more likely to be obscured in the presence of noise. An additional cause of confusion is that P waves can be absent, replaced by fibrillatory or flutter waves, or even hidden within the T waves or QRS complex, depending on which arrhythmia event is occurring. When it comes to correct detection, identifying P waves can therefore prove to be a bigger challenge than detecting QRS and T waves.

To deal with the problem of imbalanced difficulty between classes, we adopt focal loss as introduced in [31] as our segmentation loss function. Focal loss modifies the standard cross-entropy loss by providing smaller weights to well-classified time stamps, letting the model focus on regions that are difficult to classify. The focal loss generalized to our multi-class segmentation setting can be written in the following form:

$$\mathcal{L}_{\text{focal}} = -\frac{1}{N} \sum_{n=1}^N \sum_{c=1}^C (1 - \hat{y}_{n,c})^{\gamma} y_{n,c} \log \hat{y}_{n,c}$$

Here, $\hat{y}_{n,c}$ denotes the predicted probability of time stamp n belonging to class c , while y_n is the one-hot vector of the true class label for time stamp n . In our experiments, we use the default value of $\gamma = 1.0$. During arrhythmia classification guidance of Section 3.2, we use the standard binary cross-entropy loss \mathcal{L}_{bce} for the classification branch. This gives the overall loss function:

$$\mathcal{L}_{\text{total}} = \mathcal{L}_{\text{focal}} + \alpha \mathcal{L}_{\text{bce}}.$$

The additional trade-off parameter α can be adjusted to balance the effect of classification and segmentation losses during training. For all our experiments, we used $\alpha = 1$.

3.4. Training. We have trained the network from scratch with convolutional weights initialized as in He et al. [32] using the Adam optimizer [33] with default parameters. The learning rate was initialized to be 0.001 and set to follow a cosine annealing schedule. During training, we randomly applied data augmentation including transformations designed to mimic probable physiological noise, such as baseline wander, powerline noise, and baseline shift, as used in [34]. We have also randomly resized the input signal and added random Gaussian noise. Figure 5 shows examples of the used transformations.

4. DATA

For this study, we have used both internal and external public datasets for the purposes of training and validation of our model. The descriptions for both these datasets are shown in Table 1, and are explained in the following sections.

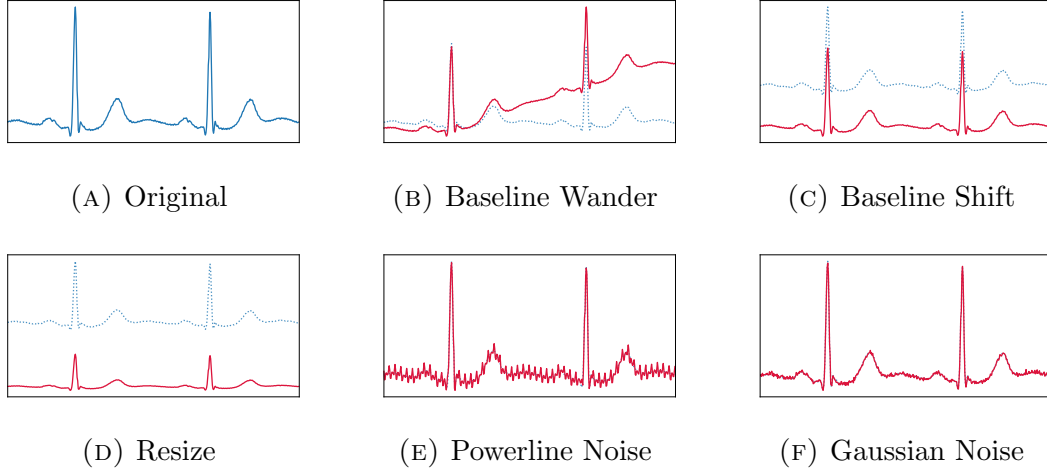


FIGURE 5. Examples of transformations used for data augmentation.

4.1. Internal Dataset. We have assembled an internal database of ECG signals from 1,557 patients by searching the electrocardiography database (GE MUSE, GE Healthcare, Wauke-sha, WI) in a single center (Seoul National University Hospital, Seoul, South Korea). In the process of ECG extraction, all personal information was anonymized, so the consent form was waived. This study was then approved by the institutional review board of the participating center (H-1906-163-1044).

Our intent was to collect a dataset in order to conduct experiments to elucidate the segmentation performance for signals during arrhythmia. To do so, we identified 155 patients with Atrial Fibrillation(AFIB) and 59 with Atrial Flutter(AFL). Among the rest, arrhythmia types were identified for 490 patients as normal sinus rhythm (NSR), 84 as sinus tachycardia (ST), 115 as bundle branch block (BBB), 197 as first degree atrioventricular block (AVB1) and 29 as ventricular tachycardia (VT).

For each patient, the extracted data consisted of a recording with a duration of 10 seconds for leads I and II with a sampling frequency of either 250Hz or 500Hz. The onsets and offsets for P, QRS and T waves were annotated for each lead independently. The dataset was partitioned into a training set and a test set. The training set comprised 1032 patients and was organized to include approximately 70% of patients for each identified arrhythmia class. The test set was composed of the remaining 525 patients.

4.2. Lobachevsky University Database(LUDB). For external validation of our methods, we evaluated our model on an open access dataset, the Lobachevsky University Database (LUDB) [12], which is available on Physionet. We chose this database since it has a complete set of annotations for all onsets and offsets of P, QRS and T waves, which are included for each single lead signal. The LUDB dataset has been used in the previous studies [4, 11, 27] as a standard database for evaluation of ECG delineation algorithms, allowing for a comparison with existing deep learning methods. The dataset contains 12-leads ECG signals from 200 unique patients. For each lead, a signal of 500Hz is recorded for a duration of 10 seconds.

4.3. Preprocessing. We train and validate our model using single lead ECG signals. As noted in [11], the first and last cardiac cycles are not annotated in the LUDB dataset, while the first and last marked segments necessarily correspond to QRS waves. We take

this into account by cropping the first and last 2 seconds of our signals during the training process. Hence, our model performs segmentation and classification using a signal of duration 6 seconds during training, and of 10 seconds during validation. While this scheme was designed mainly due to its practicality, we note that ECG recordings of 5 or 10 seconds have been shown to be successful for a CNN based arrhythmia classification [35]. We only use signals from leads I and II for training and validation of our model. Each input signal is resampled to 500Hz.

5. RESULTS

5.1. Evaluation Metrics. To evaluate the performance of our model, we compare the ground truth annotations for the onsets and offsets of P, QRS and T waves with the predicted annotations. To ensure soundness, we follow the usual standard chosen by The Association for the Advancement of Medical Instrumentation(AAMI) [36], which considers an onset or an offset to be correctly detected if an algorithm locates the same type of annotation in a neighborhood of 150ms. Using this threshold value, we examine for each predicted point whether the prediction correctly detects a point in the ground truth annotation.

If a ground truth annotation is correctly detected, we count a true positive(TP). In this case, the error is measured as the time deviation of the predicted point from the manual annotation. If there is no point of the ground truth annotation in the 150ms neighborhood of the prediction, then we count a false positive(FP). Once every prediction has been compared with the manual labels, we count for each point of the ground truth annotation which has not been related to any prediction a false negative(FN).

Based on this, we calculate the following evaluation metrics:

- mean error m
- standard deviation of error σ
- sensitivity

$$Se = \frac{TP}{TP + FN}$$

- positive predictive value

$$PPV = \frac{TP}{TP + FP}$$

- F1-score

$$F1 = 2 \cdot \frac{Se \cdot PPV}{Se + PPV}$$

These metrics have been commonly used in the literature for the evaluation of ECG delineation algorithms [4, 11, 27, 37]. In the following sections, we use these metrics to evaluate the performance of our model and draw comparisons with existing models.

5.2. Improved Segmentation on Arrhythmia. The performance of ECG segmentation models on different arrhythmia classes has rarely been explored in the literature, although the recent paper by Saclova et al. [13] presents the situation of an advanced rule-based approach. In this section, we investigate the performance of our model in accurately delineating signals exhibiting various arrhythmias. We conduct separate evaluations on different rhythm types, including normal sinus rhythm (NSR), sinus tachycardia (ST), bundle branch block (BBB), first degree atrioventricular block (AVB1), atrial fibrillation (AFIB), atrial flutter (AFL), and ventricular tachycardia (VT). To examine how the diversity of arrhythmia in the training set affects the model performance, we compare the results to the model trained solely on the

Training	Rhythm	F1-scores (%)					
		P onset	P offset	QRS onset	QRS offset	T onset	T offset
Trained on LUDB	NSR	99.84	99.84	99.83	99.84	99.97	99.97
	ST	81.54	81.54	99.93	99.93	97.59	98.83
	BBB	98.89	98.89	99.94	99.94	99.89	99.94
	AVB1	90.53	90.97	99.82	99.82	100.00	100.00
	AFIB	-	-	99.29	99.29	97.92	97.60
	AFL	-	-	99.21	99.21	92.67	93.00
	VT	-	-	91.04	91.11	78.78	78.63
	All	90.37	90.46	99.45	99.46	97.42	97.54
Trained w/o classification	NSR	99.69	99.69	99.78	99.81	99.95	99.95
	ST	97.19	97.19	99.91	99.91	99.90	99.94
	BBB	99.00	99.00	99.94	99.94	99.88	99.89
	AVB1	95.93	95.93	99.84	99.84	100.00	100.00
	AFIB	-	-	99.54	99.54	99.56	99.54
	AFL	-	-	98.97	98.97	98.56	97.57
	VT	-	-	97.83	96.84	94.49	94.61
	All	96.47	96.46	99.71	99.69	99.67	99.63
Trained w/ classification	NSR	99.61	99.61	99.82	99.84	99.95	99.95
	ST	97.04	97.04	99.91	99.91	99.80	99.89
	BBB	98.95	98.95	99.94	99.94	99.90	99.90
	AVB1	95.77	95.77	99.84	99.84	100.00	100.00
	AFIB	-	-	99.55	99.56	99.61	99.72
	AFL	-	-	99.13	99.14	98.44	97.28
	VT	-	-	97.29	97.43	92.25	94.93
	All	96.97	96.97	99.72	99.73	99.53	99.56

TABLE 2. Performance evaluated on the internal dataset. The F1-scores are averaged over 20 runs.

LUDB dataset. While the number of records is limited to 200, LUDB comes with separate annotations for all 12 leads which provide sufficient amount of data for training when treated individually.

Table 2 shows the F1-score performance of the model for three training strategies: training solely on LUDB signals, and training on the internal dataset with and without arrhythmia classification guidance (Section 3.2). The models trained on the internal dataset exhibit high F1-scores (all above 0.97, except for P waves for AVB1 and VT) across all arrhythmia types, which can be attributed to the balanced training set with sufficient samples for each arrhythmia type. In contrast, the performance of the model trained on LUDB varies significantly across different rhythm types. Although the model achieves exceptional F1-scores (over 0.99) for normal sinus rhythm, the overall performance is substantially lower, particularly for P and T wave delineation. Specifically, the scores are comparatively lower for P waves during ST and AVB1, and T waves during ST, AFIB, AFL, and VT. For BBB, the effect is not noticeable in the F1 scores, but we observed a substantial improvement in the mean and standard deviation of error for QRS offset and T onset delineation.

The relatively lower performance when training only with LUDB can be attributed to the limited number of patients in LUDB for the corresponding rhythm types. For example, only four subjects with sinus tachycardia and three subjects with atrial flutter are available [12]. These observations highlight the importance of using a well-curated dataset that encompasses

	AFIB (1437 beats)		AFL (540 beats)		All (14418 beats)			
	False Positives		False Positives		<i>PPV</i> (Precision)		<i>Se</i> (Recall)	
	P onset	P offset	P onset	P offset	P onset	P offset	P onset	P offset
Trained w/o classification	62.35	62.35	34.25	34.25	97.53	97.52	95.43	95.43
Trained w/ classification	13.85	13.85	1.85	1.9	98.70	98.69	95.31	95.31

TABLE 3. Number of false positive P annotations for AFIB and AFL. The *PPV* and *Se* scores for the entire test set are shown for reference. The values are averaged over 20 runs.

a broad range of rhythms commonly seen in clinical practice for training and validating an ECG delineation algorithm.

The model’s performances trained with and without arrhythmia classification guidance are comparable with a slight improvement observed in P wave delineation. The effect of classification guidance on P wave delineation during atrial fibrillation and atrial flutter is more properly studied in the subsequent section.

5.3. Reduced False P wave Predictions. The arrhythmia classification guidance was presented in Section 3.2 as a method with the potential benefit of reducing the number of false P wave detections which occur frequently during atrial fibrillation and flutter events. To evaluate its effectiveness, we compared the number of false positive P wave predictions generated by models trained with and without classification guidance. Table 3 shows the results, including the *PPV* and *Se* scores for the entire test set as a reference.

The results indicate a significant reduction in false positives for both atrial fibrillation and atrial flutter. When compared to the total number of beats corresponding to the same rhythm type (indicated in the header row of Table 3), the number of false positives for the classification guided model is less than 1%. The reduction in false predictions is reflected in the improved *PPV* scores for P waves belonging to the entire test set, while recall scores only decreased slightly. As a result, the total F1-score increased from 96.47% to 96.97%, as reported in Table 2.

5.4. External Validation on LUDB. To evaluate the generalizability of our model, which was trained solely on our internal training set, we tested it on signals from LUDB and compared its performance with one of the best delineation algorithms using wavelets [4] and previous deep learning based segmentation methods [11,27]. We used the standard evaluation metrics explained in Section 5.1, and the results are presented in Table 4.

Our proposed method exhibited comparable performance in terms of both F1-score and standard deviation of error. Notably, we achieved this level of performance using a training set that was entirely separate from LUDB. This sets our approach apart from previous deep-learning methods, where either LUDB was partitioned into training and test sets [27] or an extended version of LUDB was used for training [11]. The results indicate the high generalization capabilities of our model, and deep learning based ECG segmentation models in general, which can reliably be applied to an unseen collection of signals without the need for adjusting extra parameters.

		P onset	P offset	QRS onset	QRS offset	T onset	T offset
Kalyakulina <i>et al.</i> [4]	<i>Se</i> (%)	98.46	98.46	99.61	99.61	-	98.03
	<i>PPV</i> (%)	96.41	96.41	99.87	99.87		98.84
	F1 (%)	97.42	97.42	99.74	99.74		98.43
	$m \pm \sigma$ (ms)	-2.7 ± 10.2	0.4 ± 11.4	-8.1 ± 7.7	3.8 ± 8.8		5.7 ± 15.5
Sereda <i>et al.</i> [27]	<i>Se</i> (%)	95.20	95.39	99.51	99.50	97.95	97.56
	<i>PPV</i> (%)	82.66	82.59	98.17	97.96	94.81	94.96
	F1 (%)	88.49	88.53	98.84	98.72	96.35	96.24
	$m \pm \sigma$ (ms)	2.7 ± 21.9	-7.4 ± 28.6	2.6 ± 12.4	-1.7 ± 14.1	8.4 ± 28.2	-3.1 ± 28.2
Moskalenko <i>et al.</i> [11]	<i>Se</i> (%)	98.61	98.59	99.99	99.99	99.32	99.40
	<i>PPV</i> (%)	95.61	95.59	99.99	99.99	99.02	99.10
	F1 (%)	97.09	97.07	99.99	99.99	99.17	99.25
	$m \pm \sigma$ (ms)	-4.1 ± 20.4	3.7 ± 19.6	1.8 ± 13.0	-0.2 ± 11.4	-3.6 ± 28.0	-4.1 ± 35.3
Our Method (w/o classification)	<i>Se</i> (%)	98.16	98.20	99.67	99.97	99.82	99.63
	<i>PPV</i> (%)	96.39	96.36	99.29	99.59	99.66	99.42
	F1 (%)	97.27	97.27	99.48	99.78	99.74	99.52
	$m \pm \sigma$ (ms)	7.4 ± 14.1	-1.8 ± 9.9	6.1 ± 10.5	2.0 ± 10.7	3.0 ± 25.2	4.5 ± 24.4
Our Method (w/ classification)	<i>Se</i> (%)	97.98	98.05	99.69	100.00	99.82	99.54
	<i>PPV</i> (%)	97.18	97.21	99.35	99.65	99.63	99.33
	F1 (%)	97.58	97.63	99.52	99.82	99.72	99.43
	$m \pm \sigma$ (ms)	7.2 ± 13.9	-1.0 ± 9.6	6.7 ± 10.6	-1.2 ± 11.6	3.4 ± 25.0	3.3 ± 25.6

TABLE 4. Comparison of delineation performance on LUDB. For a direct comparison, we have considered the results of Moskalenko *et al.* [11] which uses single lead input, namely lead II.

5.5. Examples of Segmentation Results. This section presents examples of our model’s segmentation outcomes on the MIT-BIH arrhythmia database [18]. We have chosen multiple instances of arrhythmia to showcase how our model handles them, as depicted in Figure 6. Other challenges are shown in Figure 7, including noise, baseline wander, and loss of signal. Notably, our model achieves high accuracy in all of these examples without the need for any signal preprocessing. The results demonstrate how deep segmentation models can effectively handle the challenges presented by abnormal rhythm and noise, given a training set that comprises various rhythm types and data augmentation techniques that consider noise.

6. DISCUSSION

A deep learning based segmentation model was developed to detect the onsets and offsets of P, QRS and T waves. Our evaluation of the model on our internal dataset revealed that the quality of annotation in a segmentation model is significantly affected by the presence of arrhythmias. This observation aligns with previous research, such as the study by Saclova *et al.* [13], which also highlighted differences in annotation quality in a rule-based approach. Overall, our findings underscore the importance of accounting for arrhythmias when developing and evaluating segmentation models for ECG analysis. To address this issue, we have proposed a classification-guided segmentation model. We observed that this approach reduces the number of false positives for P waves while maintaining high accuracy on the LUDB dataset. In combination with a larger and more diverse training set, the gap between the delineation performance for different types of arrhythmia has been narrowed.

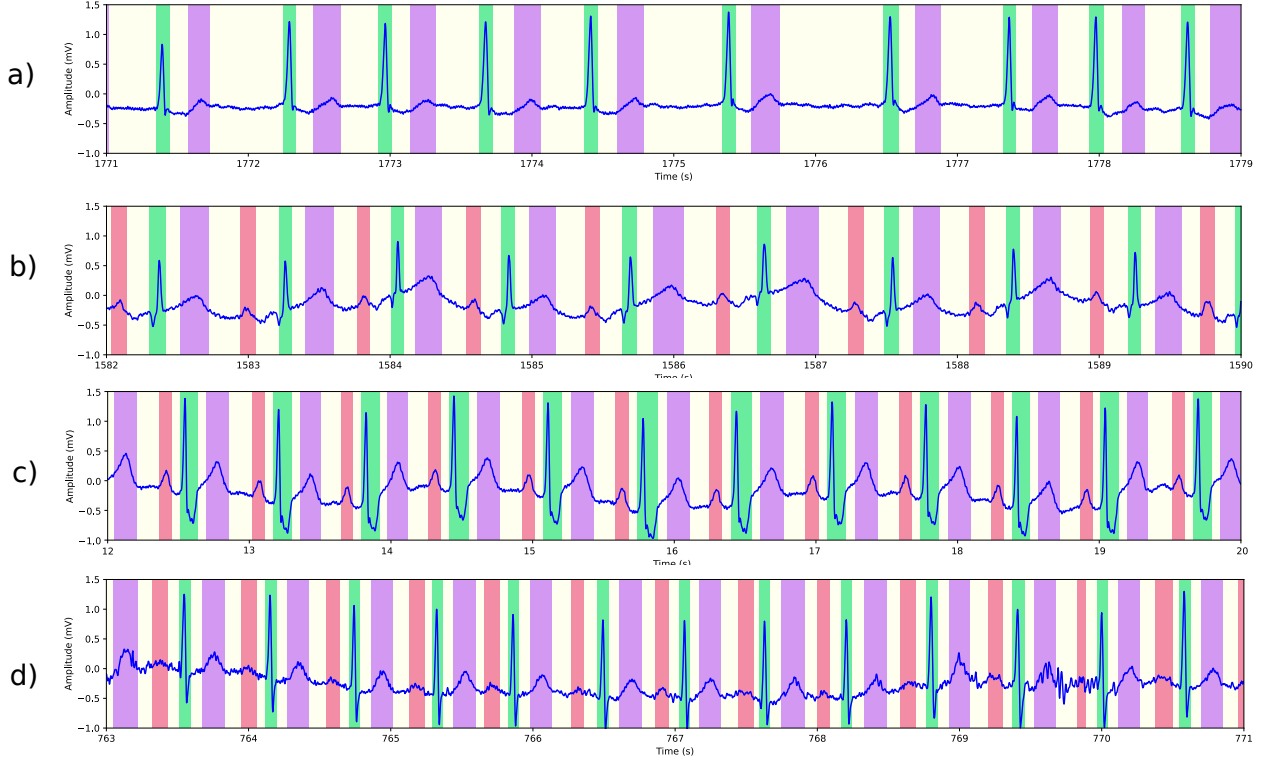


FIGURE 6. Segmentation results on the MIT-BIH arrhythmia database. (a) Atrial fibrillation in record 221. The small bumps are not misidentified as P waves, and we have observed the same correct behavior in the presence of atrial flutter. (b) First degree atrioventricular block in record 228, with correct detection of longer-than-normal PR intervals. (c) Bundle branch block in record 212, featuring a wide QRS complex. (d) Sinus tachycardia in record 209, with heart rate slightly over 100 bpm.

Moreover, as is evident from the examples from Section 5.5, our model is robust to noise and other artifacts such as baseline wander due to data augmentation techniques.

Our study has some limitations. Specifically, both our internal dataset and the LUDB dataset used as our test set have a somewhat limited diversity of arrhythmias. To the best of our knowledge, there are no other publicly available datasets with complete annotations of onset and offset data that cover a wider range of arrhythmias. To address this limitation, future research and development could focus on expanding the development and testing of automatic delineation in a broader class of arrhythmias. A particular area for improvement could be P wave detection, especially in cases of complete atrioventricular block where the P wave can occur anywhere. More manual annotation to serve as training data is not a feasible approach, particularly in cases of complete AV block. Instead, more advanced data augmentation techniques hold promise for enhancing model performance in these scenarios.

REFERENCES

- [1] Adam Gacek and Witold Pedrycz, editors. *ECG Signal Processing, Classification and Interpretation: A Comprehensive Framework of Computational Intelligence*. Springer London, London, 2012.

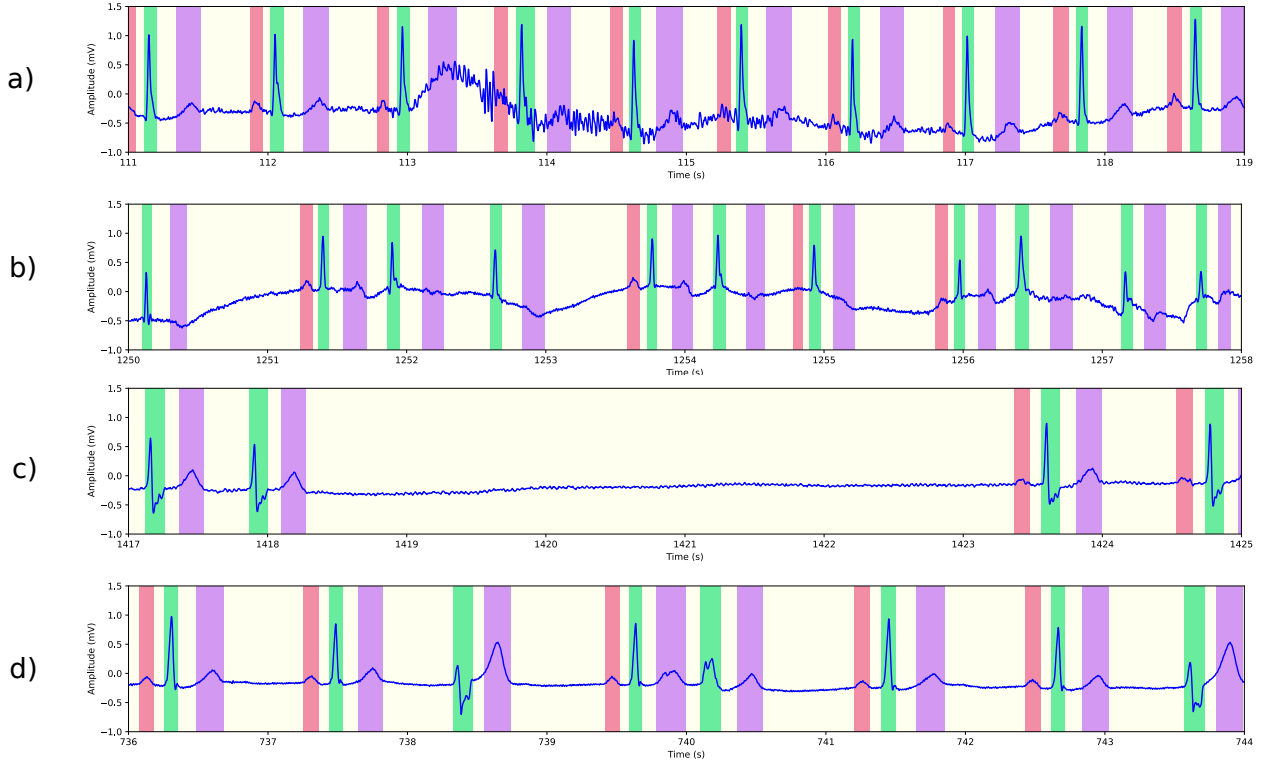


FIGURE 7. More segmentation results on the MIT-BIH arrhythmia database. (a) Normal sinus rhythm in record 101, with baseline oscillations and noise. (b) The onset of an episode of atrial flutter in record 222. The early signal displays normal sinus rhythm with PAC, and P waves being detected. Later, atrial flutter without P waves is observed. (c) An episode of loss of signal in record 232. (d) Ventricular trigeminy in record 201.

- [2] Cuiwei Li, Chongxun Zheng, and Changfeng Tai. Detection of ECG characteristic points using wavelet transforms. *IEEE Transactions on Biomedical Engineering*, 42(1):21–28, January 1995.
- [3] J.P. Martinez, R. Almeida, S. Olmos, A.P. Rocha, and P. Laguna. A Wavelet-Based ECG Delineator: Evaluation on Standard Databases. *IEEE Transactions on Biomedical Engineering*, 51(4):570–581, April 2004.
- [4] A. I. Kalyakulina, I. I. Yusipov, V. A. Moskalenko, A. V. Nikolskiy, A. A. Kozlov, N. Yu. Zolotikh, and M. V. Ivanchenko. Finding Morphology Points of Electrocardiographic-Signal Waves Using Wavelet Analysis. *Radiophysics and Quantum Electronics*, 61(8):689–703, January 2019.
- [5] P. Laguna, R.G. Mark, A. Goldberg, and G.B. Moody. A database for evaluation of algorithms for measurement of QT and other waveform intervals in the ECG. In *Computers in Cardiology 1997*, pages 673–676, Lund, Sweden, 1997. IEEE.
- [6] Guillermo Jimenez-Perez, Alejandro Alcaine, and Oscar Camara. Delineation of the electrocardiogram with a mixed-quality-annotations dataset using convolutional neural networks. *Scientific Reports*, 11(1):863, January 2021.
- [7] Zhenqin Chen, Mengying Wang, Meiyu Zhang, Wei Huang, Hanjie Gu, and Jinshan Xu. Post-processing refined ECG delineation based on 1D-UNet. *Biomedical Signal Processing and Control*, 79:104106, January 2023.
- [8] Awni Y. Hannun, Pranav Rajpurkar, Masoumeh Haghpanahi, Geoffrey H. Tison, Codie Bourn, Mintu P. Turakhia, and Andrew Y. Ng. Cardiologist-level arrhythmia detection and classification in ambulatory electrocardiograms using a deep neural network. *Nature Medicine*, 25(1):65–69, January 2019.

- [9] Wen Hao and Kang Jingsu. Investigating Deep Learning Benchmarks for Electrocardiography Signal Processing, April 2022. arXiv:2204.04420 [cs].
- [10] Olaf Ronneberger, Philipp Fischer, and Thomas Brox. U-Net: Convolutional Networks for Biomedical Image Segmentation. In Nassir Navab, Joachim Hornegger, William M. Wells, and Alejandro F. Frangi, editors, *Medical Image Computing and Computer-Assisted Intervention – MICCAI 2015*, volume 9351, pages 234–241. Springer International Publishing, Cham, 2015.
- [11] Viktor Moskalenko, Nikolai Zolotykh, and Grigory Osipov. Deep Learning for ECG Segmentation. In Boris Kryzhanovsky, Witali Dunin-Barkowski, Vladimir Redko, and Yury Tiumentsev, editors, *Advances in Neural Computation, Machine Learning, and Cognitive Research III*, volume 856, pages 246–254. Springer International Publishing, Cham, 2020.
- [12] Alena I. Kalyakulina, Igor I. Yusipov, Viktor A. Moskalenko, Alexander V. Nikolskiy, Konstantin A. Kosonogov, Grigory V. Osipov, Nikolai Yu. Zolotykh, and Mikhail V. Ivanchenko. LUDB: A New Open-Access Validation Tool for Electrocardiogram Delineation Algorithms. *IEEE Access*, 8:186181–186190, 2020.
- [13] Lucie Saclova, Andrea Nemcova, Radovan Smisek, Lukas Smital, Martin Vitek, and Marina Ronzhina. Reliable P wave detection in pathological ECG signals. *Scientific Reports*, 12(1):6589, April 2022.
- [14] Jianyuan Hong, Hua-Jung Li, Chung-chi Yang, Chih-Lu Han, and Jui-chien Hsieh. A clinical study on Atrial Fibrillation, Premature Ventricular Contraction, and Premature Atrial Contraction screening based on an ECG deep learning model. *Applied Soft Computing*, 126:109213, September 2022.
- [15] Saira Aziz, Sajid Ahmed, and Mohamed-Slim Alouini. ECG-based machine-learning algorithms for heart-beat classification. *Sci. Rep.*, 11(1):18738, September 2021.
- [16] Huimin Huang, Lanfen Lin, Ruofeng Tong, Hongjie Hu, Qiaowei Zhang, Yutaro Iwamoto, Xianhua Han, Yen-Wei Chen, and Jian Wu. UNet 3+: A Full-Scale Connected UNet for Medical Image Segmentation. In *ICASSP 2020 - 2020 IEEE International Conference on Acoustics, Speech and Signal Processing (ICASSP)*, pages 1055–1059, Barcelona, Spain, May 2020. IEEE.
- [17] Md. Badiuzzaman Shuvo, Rifat Ahommed, Sakib Reza, and M.M.A. Hashem. CNL-UNet: A novel lightweight deep learning architecture for multimodal biomedical image segmentation with false output suppression. *Biomedical Signal Processing and Control*, 70:102959, September 2021.
- [18] G. B. Moody and R. G. Mark. The impact of the MIT-BIH arrhythmia database. *IEEE engineering in medicine and biology magazine: the quarterly magazine of the Engineering in Medicine & Biology Society*, 20(3):45–50, 2001.
- [19] Jiapu Pan and Willis J. Tompkins. A Real-Time QRS Detection Algorithm. *IEEE Transactions on Biomedical Engineering*, BME-32(3):230–236, March 1985.
- [20] D.S. Benitez, P.A. Gaydecki, A. Zaidi, and A.P. Fitzpatrick. A new QRS detection algorithm based on the Hilbert transform. In *Computers in Cardiology 2000. Vol.27 (Cat. 00CH37163)*, pages 379–382, September 2000.
- [21] S. K. Mukhopadhyay, M. Mitra, and S. Mitra. Time plane ECG feature extraction using Hilbert transform, variable threshold and slope reversal approach. In *2011 International Conference on Communication and Industrial Application*, pages 1–4, December 2011.
- [22] A Martínez, R Alcaraz, and J J Rieta. Automatic electrocardiogram delineator based on the Phasor Transform of single lead recordings. In *2010 Computing in Cardiology*, pages 987–990, September 2010.
- [23] S. Graja and J.-M. Boucher. Hidden Markov tree model applied to ECG delineation. *IEEE Transactions on Instrumentation and Measurement*, 54(6):2163–2168, December 2005.
- [24] Mahsa Akhbari, Mohammad B. Shamsollahi, Omid Sayadi, Antonis A. Armoundas, and Christian Jutten. ECG segmentation and fiducial point extraction using multi hidden Markov model. *Computers in Biology and Medicine*, 79:21–29, December 2016.
- [25] Rémi Dubois, Pierre Maison-Blanche, Brigitte Quenet, and Gérard Dreyfus. Automatic ECG wave extraction in long-term recordings using Gaussian mesa function models and nonlinear probability estimators. *Computer Methods and Programs in Biomedicine*, 88(3):217–233, December 2007.
- [26] Guillermo Jimenez-Perez, Alejandro Alcaine, and Oscar Camara. U-Net Architecture for the Automatic Detection and Delineation of the Electrocardiogram. In *2019 Computing in Cardiology (CinC)*, pages Page 1–Page 4, September 2019.

- [27] Iana Sereda, Sergey Alekseev, Aleksandra Koneva, Roman Kataev, and Grigory Osipov. ECG Segmentation by Neural Networks: Errors and Correction. In *2019 International Joint Conference on Neural Networks (IJCNN)*, pages 1–7, July 2019.
- [28] Antônio H. Ribeiro, Manoel Horta Ribeiro, Gabriela M. M. Paixão, Derick M. Oliveira, Paulo R. Gomes, Jéssica A. Canazart, Milton P. S. Ferreira, Carl R. Andersson, Peter W. Macfarlane, Wagner Meira, Thomas B. Schön, and Antonio Luiz P. Ribeiro. Automatic diagnosis of the 12-lead ECG using a deep neural network. *Nature Communications*, 11(1):1760, April 2020.
- [29] Kaiming He, Xiangyu Zhang, Shaoqing Ren, and Jian Sun. Deep Residual Learning for Image Recognition. In *2016 IEEE Conference on Computer Vision and Pattern Recognition (CVPR)*, pages 770–778, Las Vegas, NV, USA, June 2016. IEEE.
- [30] Zongwei Zhou, Md Mahfuzur Rahman Siddiquee, Nima Tajbakhsh, and Jianming Liang. UNet++: Redesigning Skip Connections to Exploit Multiscale Features in Image Segmentation. *IEEE Transactions on Medical Imaging*, 39(6):1856–1867, June 2020.
- [31] Tsung-Yi Lin, Priya Goyal, Ross Girshick, Kaiming He, and Piotr Dollar. Focal loss for dense object detection. In *Proceedings of the IEEE International Conference on Computer Vision (ICCV)*, October 2017.
- [32] Kaiming He, Xiangyu Zhang, Shaoqing Ren, and Jian Sun. Delving Deep into Rectifiers: Surpassing Human-Level Performance on ImageNet Classification. In *2015 IEEE International Conference on Computer Vision (ICCV)*, pages 1026–1034, Santiago, Chile, December 2015. IEEE.
- [33] Diederik P. Kingma and Jimmy Ba. Adam: A Method for Stochastic Optimization, January 2017. arXiv:1412.6980 [cs].
- [34] Temesgen Mehari and Nils Strodthoff. Self-supervised representation learning from 12-lead ECG data. *Computers in Biology and Medicine*, 141:105114, February 2022.
- [35] Xiaomao Fan, Qihang Yao, Yunpeng Cai, Fen Miao, Fangmin Sun, and Ye Li. Multiscaled Fusion of Deep Convolutional Neural Networks for Screening Atrial Fibrillation From Single Lead Short ECG Recordings. *IEEE Journal of Biomedical and Health Informatics*, 22(6):1744–1753, November 2018.
- [36] NM Association for the Advancement of Medical Instrumentation and others. Testing and reporting performance results of cardiac rhythm and ST segment measurement algorithms. *ANSI/AAMI EC38*, 1998:46, 1998.
- [37] José Manuel Bote, Joaquín Recas, Francisco Rincón, David Atienza, and Román Hermida. A Modular Low-Complexity ECG Delineation Algorithm for Real-Time Embedded Systems. *IEEE Journal of Biomedical and Health Informatics*, 22(2):429–441, March 2018.

¹ DEPARTMENT OF MATHEMATICAL SCIENCES AND RESEARCH INSTITUTE OF MATHEMATICS, SEOUL NATIONAL UNIVERSITY, BUILDING 27, SAN 56-1, SILLIM-DONG, GWANAK-GU, SEOUL, SOUTH KOREA, POSTAL CODE 08826

² DIVISION OF CARDIOLOGY, DEPARTMENT OF INTERNAL MEDICINE, ASAN MEDICAL CENTER, UNIVERSITY OF ULSAN COLLEGE OF MEDICINE, SEOUL, SOUTH KOREA

³ AI INSTITUTE, SEOUL NATIONAL UNIVERSITY, SEOUL, SOUTH KOREA

⁴ DEPARTMENT OF SURGERY, SEOUL NATIONAL UNIVERSITY HOSPITAL AND SEOUL NATIONAL UNIVERSITY COLLEGE OF MEDICINE, SEOUL, SOUTH KOREA

⁵ DEPARTMENT OF CRITICAL CARE MEDICINE, SEOUL NATIONAL UNIVERSITY HOSPITAL

⁶ DEPARTMENT OF INTERNAL MEDICINE, SEOUL NATIONAL UNIVERSITY HOSPITAL, SEOUL, SOUTH KOREA

⁷ MEDIFARMSOFT CO., LTD., SEOUL, SOUTH KOREA